

NANOSTRUCTURES

Interwave interaction in an array of carbon nanotubes with a dynamic plasmon lattice

To cite this article: S.A. Afanas'ev *et al* 2021 *Quantum Electron.* **51** 609

View the [article online](#) for updates and enhancements.

You may also like

- [Floristry and plant biogeography of the Eastern part of the Volga Upland](#)
M M Gafurova, A V Ivanova and E Yu Istomina
- [Optical generation in an amplifying photonic crystal with metal nanoparticles](#)
I Glukhov and S Moiseev
- [Improvement of the working surface resistance of a stamping tool with coating and SSS modeling of the preliminary mechanical activation of the surface layer of the stamp working parts](#)
V P Tabakov, V N Kokorin, O I Morozov et al.

Interwave interaction in an array of carbon nanotubes with a dynamic plasmon lattice

S.A. Afanas'ev, I.O. Zolotovskii, A.S. Kadochkin, S.G. Moiseev, V.V. Svetukhin, A.A. Pavlov

Abstract. It is shown that when counterpropagating laser beams are incident on an array of parallel single-walled carbon nanotubes, strong interaction of waves is possible, accompanied by the amplification of one of the waves at the expense of another, more intense pump wave. The interaction is most efficient when the condition of phase matching of the incident waves and the slow plasmon polariton wave formed because of the laser-induced metallisation of nanotubes is satisfied. The dependence of the signal wave gain on the geometric parameters of the array and the wave characteristics of the incident waves is studied numerically. A range of phase detuning values is found, in which the gain changes weakly near its maximum value.

Keywords: single-walled carbon nanotubes, surface plasmon polaritons, coupled waves, interwave interactions, phase matching.

1. Introduction

Arrays of ordered carbon nanotubes (CNTs) and nanocomposites based on them are being intensively studied as promising objects for solving various problems related to the generation and control of electromagnetic radiation in various frequency ranges, from optical to microwave [1–9]. Technologies have been developed for producing arrays with controlled parameters, consisting of both multi-walled (MWCNT) [3–5] and single-walled (SWCNT) [6, 8, 9] tubes. CNT arrays are used to develop radiation absorbers [3, 10], thermal emitters [8, 11], signal processing devices [4, 9], terahertz and IR emitters [12, 13], etc. A number of applications is possible because a CNT can act as a transmission line (waveguide) supporting the propagation of an infraslow (with an effective refractive index of more than 100) surface electromagnetic waves [14–21].

As shown in Refs [4, 22], to describe arrays of parallel CNTs, a wire medium model can be used, which is a two-dimensional lattice of parallel thin conducting rods (wires),

well studied in connection with numerous applications in microwave technology [23–25]. This material can be considered as a uniaxial electron plasma in which free electrons can move only along the wires. The frequency dependence of the effective dielectric constant of such a medium is determined based on the Drude model for metals:

$$\varepsilon = 1 - \frac{\omega_p^2}{\omega^2 + i\nu\omega}, \quad (1)$$

where ω is the cyclic frequency, and ν is a coefficient characterising optical losses. The effective plasma frequency ω_p for a square lattice is defined as [23]

$$\omega_p^2 = \frac{2\pi c^2}{d^2 \ln(d/a)}, \quad (2)$$

where d is the lattice period, and a is the radius of the wire (nanotube).

According to Eqn (2), the effective plasma frequency depends only on the radius of the wires and the lattice period, which makes it possible to produce CNT arrays with the required ω_p value. However, at first glance, this result does not agree with the well-known formula

$$\omega_p^2 = \frac{ne^2}{m_e \varepsilon_0}, \quad (3)$$

which includes the concentration n of charge carriers, the electron mass m_e , and charge e (ε_0 is the electric constant). This means that in Eqn (3) the effective concentration of electrons and the effective mass of an electron should be used [22, 23]. The effect of inductance is interpreted as an increase in the effective electron mass, because of which the value of the plasma frequency shifts from the near UV region for bulk metals to the IR and terahertz regions for wire media and CNT arrays.

In our paper [26] we considered the mechanism of generation of slow surface plasmon polaritons (PPs) in the terahertz and far-IR ranges caused by laser irradiation of ordered arrays of SWCNTs. Under the condition of longitudinal resonance, each tube of the array with a slowed-down plasmon wave propagating in it is a dipole antenna emitting at the PP frequency. It is shown that by changing the angle of the laser beam incidence on the structure under study, it is possible to achieve matching of the length of the nanotubes in the array with the wavelength of laser sources, thereby providing optimal conditions for converting cw laser radiation into terahertz radiation. Two schemes for the implementation of this

S.A. Afanas'ev, I.O. Zolotovskii, A.S. Kadochkin, S.G. Moiseev
Ulyanovsk State University, ul. L. Tolstogo 42, 432700 Ulyanovsk,
Russia; e-mail: rafzol.14@mail.ru;
V.V. Svetukhin Scientific-Manufacturing Complex 'Technological
Centre', pl. Shokina 1, stroenie 7, Zelenograd, 124498 Moscow,
Russia; e-mail: svetukhin@mail.ru;
A.A. Pavlov Institute of Nanotechnology of Microelectronics, Russian
Academy of Sciences, Leninsky prosp. 32a, 119991 Moscow, Russia;
e-mail: alexander.a.pavlov@gmail.com

Received 13 March 2021; revision received 12 May 2021
Kvantovaya Elektronika 51 (7) 609–614 (2021)
Translated by V.L. Derbov

process are proposed. In the first case, self-decay (similar to parametric three-photon interaction in a periodic structure) of the initial laser wave into a diffracted wave and PP on the surface of nanotubes is considered. Slow PPs are excited in the array by the interaction of narrow-band laser radiation of the incident and diffracted waves with periodically located CNTs. In the second case, two laser sources with slightly different radiation frequencies are used to excite PPs in CNTs, while the generation of a slow PP is carried out at a difference frequency. The second scheme is more complicated technically, but it does not require a strict periodicity of the array of parallel CNTs. In both cases, the phase matching conditions of the corresponding wave processes must be satisfied.

In this paper, based on the two-beam scheme proposed in Ref. [26], we consider a model of the parametric interaction of input waves, a more intense pump wave at frequency ω_1 and a signal wave at frequency ω_2 . The interaction incorporates the generation of an idler wave (in our case, an infraslow PP) at the difference frequency $\Omega = \omega_1 - \omega_2$. In the simplest geometry of interaction with oppositely directed wave vectors, the phase matching condition has the form:

$$k_1(\omega_1) + k_2(\omega_2) = q(\Omega), \quad (4)$$

where $k_{1,2}$ are the propagation constants of counterpropagating collinear interacting waves, and q is the propagation constant of PPs excited in nanotubes. The condition can be met, e.g., by selecting appropriate values of the frequencies ω_1 or ω_2 . When condition (4) is fulfilled, amplification of the signal and idler waves will be most efficient. In this case, the coefficient of reflection from the structure will be close to unity at the expense of the amplified signal wave that passes through the array; however, the reflected radiation will have a frequency ω_2 that is different from the frequency ω_1 of the incident radiation.

Below we consider the situation when a high-frequency pump wave has a wavelength of $\sim 1 \mu\text{m}$, at which the most widespread and available fibre and solid-state laser sources with high average and peak powers operate. The dependence of the energy gain of the signal wave on the geometric parameters of the CNT array, as well as on the amplitude and frequency of the signal wave is investigated.

2. Statement of the problem and basic relations

We consider a two-dimensional periodic array of parallel SWCNTs of the same length L , forming a square lattice with a period d . The tubes are assumed to be long enough to satisfy the condition $d \ll L$. The array is irradiated by two counterpropagating laser beams with frequencies ω_1 and ω_2 , propagating along the axes of CNTs (z axis).

It is known that a metallic CNT can serve as a transmission line (waveguide) that ensures the propagation of a highly slowed surface electromagnetic wave [14–16, 19, 21]. If the nanotubes of the array are initially dielectric or semiconducting, then when illuminated by laser radiation, they are metallised.

Let us assume that laser radiation in the CNT array is mainly spent (lost) for the generation of PPs, which is the result of nanotube metallisation, i.e. the generation of each nonequilibrium carrier leads to the formation of a PP. Using the model of metallisation of the semiconductor surface, con-

sidered, e.g., in Ref. [27], we write an equation for the generation of nonequilibrium charges in CNTs (or, which is the same in our case, for the generation of PPs):

$$\frac{dn}{dt} \approx \frac{\alpha_1(\omega_1)}{\hbar\omega_1} I_1 + \frac{\alpha_2(\omega_2)}{\hbar\omega_2} I_2 - \frac{n}{\tau}, \quad (5)$$

where n is the volume concentration of nonequilibrium charges in one CNT; $\tau \sim 1/v_g(\Omega)\alpha_3(\Omega)$ is the lifetime of the corresponding PPs; $v_g(\Omega)$ is the group velocity of the PP; $\alpha_1(\omega_1)$, $\alpha_2(\omega_2)$, $\alpha_3(\Omega)$ are the decrements of radiation damping in CNTs at the corresponding frequency; ω_1 and I_1 are the frequency and intensity of the pump wave metallising the CNT array; and ω_2 and I_2 are the parameters of the initially low-power wave amplified by the pump wave. Below, for a rough estimate, we assume that $\alpha_1(\omega_1) \approx \alpha_2(\omega_2)$.

The concentration of nonequilibrium carriers (in our case, PPs) generated in the field of laser radiation with intensity I_1 is determined from Eqn (5) under the condition $dn/dt = 0$, $I_2 = 0$:

$$n \approx \frac{\alpha_1(\omega_1)\tau(\Omega)I_1}{\hbar\omega_1} \approx \frac{[\alpha_1(\omega_1)/\alpha_3(\Omega)]I_1}{\hbar\omega_1 v_g(\Omega)}. \quad (6)$$

Expression (6) allows obtaining the critical value I_{cr} of the laser radiation intensity at which the CNT is completely metallised. To this end, the condition $n \rightarrow n_0$ (n_0 is the charge concentration in the CNT) is used, which means that all electrons from the electrically neutral zone are ‘transferred’ to a nonequilibrium state with the formation of a surface PP. This is similar to what happens in semiconductors, when all valence electrons are ‘transferred’ to the state of nonequilibrium carriers. From Eqn (6), it follows that the intensity of the critical field is determined by the relation

$$I_{\text{cr}} \sim \hbar\omega_1 v_g(\Omega) n_0 \frac{\alpha_3(\Omega)}{\alpha_1(\omega_1)}. \quad (7)$$

For graphene at the point of electric neutrality, the surface concentration of carriers is $n_s = 2an_0 \sim 10^8 \text{ cm}^{-2}$ [28]. This allows estimating the conditions for the realisation of complete metallisation according to Eqn (7) as $I_{\text{cr}} \sim 10^4 \text{ W cm}^{-2}$ for the optical range and $I_{\text{cr}} \sim 10^3 \text{ W cm}^{-2}$ for the region near $10.6 \mu\text{m}$ (the wavelength of CO_2 lasers). The use of arrays with dense filling will make it possible to use cw narrow-band (highly coherent) laser sources with radiation intensities I_1 about 1 W cm^{-2} .

For two counterpropagating laser beams, it is possible to generate surface PPs at the difference frequency $\Omega = \omega_1 - \omega_2$ with a propagation constant $q(\Omega)$, propagating along the nanotubes. Under the assumption of complete metallisation, the dynamic component of the dielectric constant of the array [determined by expression (1)] turns out to be harmonically modulated with the frequency Ω :

$$\begin{aligned} \varepsilon_{\text{eff}} &= 1 + \Delta\varepsilon \cos[q(\Omega)z - \Omega t] \\ &= 1 - \frac{\omega_p^2}{\omega^2 + i\nu\omega} \cos[q(\Omega)z - \Omega t], \end{aligned} \quad (8)$$

where for SWCNTs the attenuation coefficient is $\nu \sim 10^{12} \text{ s}^{-1}$. Thus, a nonstationary photonic crystal is formed, providing

(under certain conditions) the interaction of two counter-propagating waves.

If $|\Delta\varepsilon| < 1$ in Eqn (8), the standard theory of coupled waves in one-dimensional periodic media [29, 30] is applicable to describe the interaction of counterpropagating waves. For $\omega_1 > \omega_2$, the interaction occurs due to the presence of a PP propagating along the CNTs in the positive direction of the z axis. In this case, for the complex amplitudes of the pump wave A_1 and the signal wave A_2 , the following system of equations is obtained:

$$\begin{aligned} \frac{dA_1}{dz} &= i\kappa_2 A_2 \exp(-i\delta z), \\ \frac{dA_2}{dz} &= -i\kappa_1 A_1 \exp(i\delta z), \end{aligned} \quad (9)$$

where $\kappa_1 = k_1^2 |\Delta\varepsilon| (\omega_1) / (4k_2)$ and $\kappa_2 = k_2^2 |\Delta\varepsilon| (\omega_2) / (4k_1)$ are the coupling coefficients; $k_{1,2}$ are the propagation constants of the counterpropagating waves (we assume that the CNTs of the array are placed in a vacuum); and $\delta = k_1 + k_2 - q$ is the phase matching detuning.

The solution of Eqns (9) shows that the result of energy exchange between coupled waves can be an increase in the amplitude A_2 of the signal wave at the expense of the high-frequency pump wave with a frequency ω_1 , i.e., parametric frequency conversion takes place. The efficiency of this process is characterised by the gain G of the signal wave intensity:

$$G = \frac{|A_2(L)|^2}{|A_2(0)|^2}. \quad (10)$$

The system of linear equations (9) has the analytical solution [30]:

$$\begin{aligned} A_1(z) &= [C_1 \exp(-\gamma z) + C_2 \exp(\gamma z)] \exp(-i\delta z/2), \\ A_2(z) &= [\beta_1 C_1 \exp(-\gamma z) + \beta_2 C_2 \exp(\gamma z)] \exp(i\delta z/2), \end{aligned} \quad (11)$$

where $\gamma = (\kappa_1 \kappa_2 - \delta^2/4)^{1/2}$; $\beta_1 = i\kappa_1 / (\gamma - \delta/2)$; and $\beta_2 = \kappa_1 / (\beta_1 \kappa_2)$. Arbitrary constants $C_{1,2}$ in Eqns (11) are found from the boundary conditions $A_1(0) = A_{10}$ and $A_2(L) = A_{20}$, specified by the amplitudes of incident waves at the array input:

$$\begin{aligned} C_1 &= -\xi [\beta_2 A_{10} \exp(\gamma L) - A_{20} \exp(-i\delta L/2)], \\ C_2 &= \xi [\beta_1 A_{10} \exp(-\gamma L) - A_{20} \exp(-i\delta L/2)], \end{aligned} \quad (12)$$

where $\xi = [\beta_1 \exp(-\gamma L) - \beta_2 \exp(\gamma L)]^{-1}$. Below, the amplitudes $A_{1,2}$ are expressed in relative units: the amplitude A_{10} of the pump wave at the array input (plane $z = 0$) is assumed to be equal to unity, and its initial phase is taken to be zero. The input signal wave amplitude in the $z = L$ plane is $A_{20} = \eta A_{10}$.

For a numerical analysis of solution (11), it is necessary to know a dispersion relation, i.e., the dependence $q(\Omega)$ for the propagation constant of a PP propagating along the tubes. The existing approaches to solving the electrodynamic problem of the surface wave propagation in a waveguide formed by CNTs [15–17, 31–33] are different, but the resulting dispersion dependences $q(\Omega)$ are in good agreement with each other. Within the framework of the hydrodynamic approach [16, 17, 31] SWCNTs are modelled by an infinitely long and

infinitely thin cylindrical shell of radius a , whose valence electrons are considered as an electron gas uniformly distributed along a cylindrical surface with a surface density n_s . A uniformly distributed electron gas interacts with the electromagnetic wave and can be considered as a charged continuous medium. As the solution obtained within this approximation shows, both pure TE and TM waves and hybrid modes can propagate in CNTs.

In the present work, we use the dispersion relation $q(\Omega)$ for a surface TM wave in a metallic SWCNT given in Ref. [17]:

$$i\Omega\varepsilon_0 = \sigma_{zz} q^2 a I(qa) K(qa), \quad (13)$$

where $I(qa)$ and $K(qa)$ are modified Bessel functions of the first and second kinds. The longitudinal component of the conductivity tensor of a metallic SWCNT is expressed as

$$\sigma_{zz} = \frac{in_s e^2}{m_e} \frac{\omega(\omega + i\nu) - \chi m^2/a^2}{(\omega + i\nu)[\omega(\omega + i\nu) - \chi q_m^2]}, \quad (14)$$

where $q_m^2 = q^2 + m^2/a^2$; m is the guided mode number; $\chi = \pi n_s \hbar^2 / m_e^2$ is the square of the wave propagation velocity in a homogeneous electronic continuous medium; and ν is the coefficient of attenuation of the electron wave, caused by the scattering of electrons by positively charged ions. Since in SWCNTs the ballistic regime is realised for the motion of electrons, their scattering by positively charged ions can be ignored. For the ratio n_s/m_e in Eqn (14), the following estimate was obtained in [34]: $n_s/m_e = 2V_F / (\pi^2 \hbar a)$, where the Fermi velocity V_F for metallic SWCNTs is estimated at $\sim 10^6$ m s⁻¹.

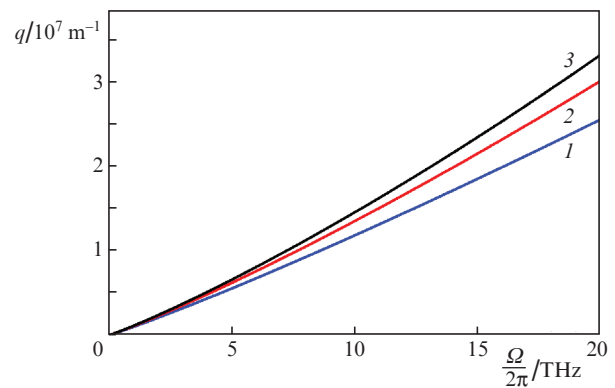


Figure 1. Frequency dependences of the PP propagation constant in metallic SWCNTs with radii $a = (1)$ 0.5, (2) 1.5, and (3) 2.5 nm.

The dispersion dependences $q(\Omega)$ obtained from Eqn (13) for tubes of different radii are shown in Fig. 1. It can be seen that the propagation constant of PPs in CNTs is $\sim 10^7$ m⁻¹, which makes it possible to satisfy the phase matching condition (4), since for the considered wavelength $\lambda_1 = 1$ μ m the wavenumber in vacuum is $k_1 = 6.28 \times 10^6$ m⁻¹. In further calculations, the dependence $q(\Omega)$ calculated for SWCNTs with a radius of 1.5 nm is used.

3. Results of numerical analysis

This section analyses the results of calculations of the gain G for the signal wave based on relations (10)–(12). In the calcu-

lations, the parameters of the SWCNT array, namely, the length L and the effective plasma frequency ω_p could be varied, as well as the frequency ω_2 and the input amplitude A_{20} of the signal wave. Variation of ω_2 (at a fixed frequency ω_1) leads to a change in the value of the detuning δ from phase matching.

It follows from Fig. 2 that the gain G substantially depends on the effective plasma frequency ω_p of the SWCNT array. It can be expected that amplification of the signal wave will be most efficient when the phase matching condition (4) is fulfilled as accurately as possible, i.e., at $\delta \rightarrow 0$. The dependences in Fig. 2a are plotted for $\lambda_2 = 1.032 \mu\text{m}$, which corresponds to a small parameter of phase-matching detuning, $\delta/k_1 = 0.01$. It can be seen that in the case of a sufficiently long interaction length L , exceeding $\sim 5 \mu\text{m}$, as the parameter ω_p increases, the gain gradually saturates, reaching its maximum value. The plasma frequency value corresponding to reaching 'saturation' depends on the length of the tubes in the array, but this dependence becomes weaker if the length L exceeds $\sim 10 \mu\text{m}$.

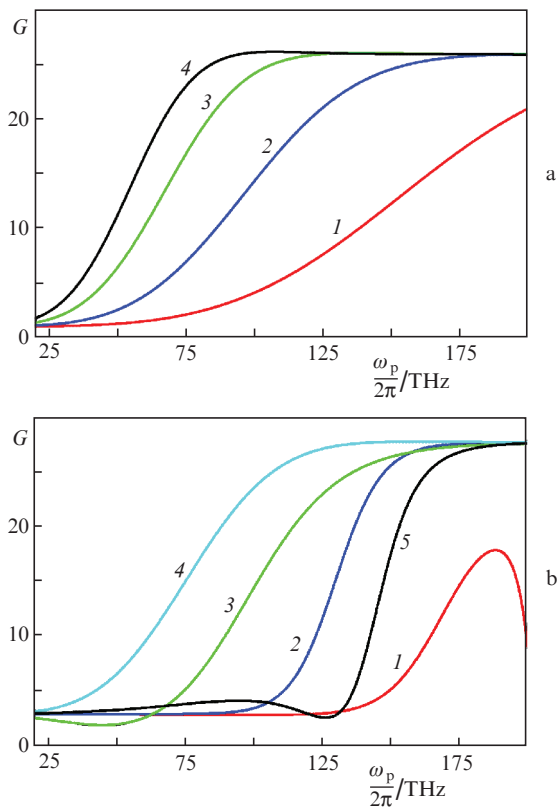


Figure 2. Dependences of the gain on the effective plasma frequency of the SWCNT array (a) at $\delta = 0.01$ and $L = (1) 2, (2) 5, (3) 10, (4) 15 \mu\text{m}$, as well as (b) at $L = 8 \mu\text{m}$ and $\delta/k_1 = (1) -0.3, (2) -0.1, (3) -0.06, (4) 0.01, (5) 0.15$. The relative amplitude of the signal wave is $\eta = 0.2$.

Since the phase matching condition is almost never exactly satisfied, it is of interest to study the dependence of the gain G on the parameter δ . Curves (1–5) in Fig. 2b are plotted at a fixed $L = 8 \mu\text{m}$ for $\lambda_2 = 1.028, 1.030, 1.031, 1.032,$ and $1.034 \mu\text{m}$. They correspond to the relative detunings $\delta/k_1 = -0.3, -0.1, -0.06, 0.01,$ and 0.15 . It can be seen that as the

absolute value of the detuning decreases, the saturation region expands significantly. At the same time, for large deviations from the phase matching regime, saturation may be absent [curve (1)].

As follows from the dependences shown in Fig. 2, to achieve the maximum effect, the array must have a sufficiently large effective plasma frequency $f_p = \omega_p/2\pi$, no less than 100 THz. For arrays of parallel MWCNTs, the values of ~ 200 THz were confirmed experimentally [4], and the results of this experiment fully agree with the calculations of the plasma frequency by formula (2) for a wire metamaterial. It can be assumed that for arrays formed by SWCNTs, formula (2) should be fulfilled even more accurately due to a significantly smaller radius of the tubes. Figure 3 shows the results of calculating the effective plasma frequency by Eqn (2) for arrays formed by SWCNTs of different radii. It can be seen that the required values $f_p \approx 100\text{--}200$ THz are achieved for sufficiently rarefied arrays with a lattice period of more than 200 nm. For further calculations, we chose $f_p = 150$ THz.

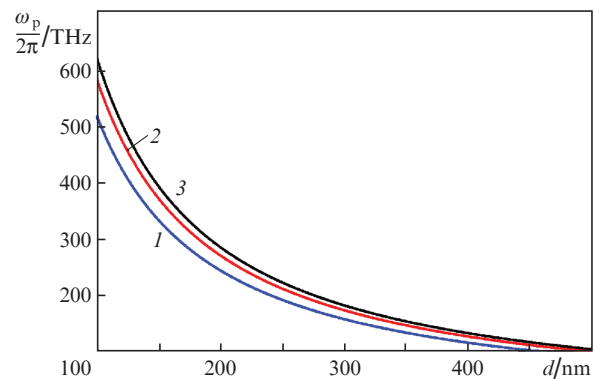


Figure 3. Effective plasma frequency of the SWCNT array as a function of the structure period d for CNTs with radii $a = (1) 0.5, (2) 1.5,$ and $(3) 2.5$ nm.

The calculations for Fig. 3 were performed under the assumption of complete metallisation of the array nanotubes, i.e., $I_1 > I_{cr}$. Since, according to (3), the plasma frequency depends on the concentration of nonequilibrium carriers, for $I_1 \leq I_{cr}$ one can write

$$\omega_p^* \approx \sqrt{n/n_0} \omega_p \approx \sqrt{I_1/I_{cr}} \omega_p \text{ for } I_1 \leq I_{cr}. \quad (15)$$

Thus, the above f_p values can also be achieved for intensities insufficient for complete metallisation by increasing the concentration of nanotubes in the array.

Dependences (11) of the amplitudes of counterpropagating waves within the array, as well as the gain (10), are composite functions of the phase detuning parameter δ . The dependences of the gain G on the normalised value δ/k_1 shown in Fig. 4 are asymmetric with respect to the $\delta = 0$ axis and near this value have a region of the highest G , the width of which depends on the length of the tubes of the array. When δ sufficiently differs from zero, the dependence $G(\delta)$ becomes oscillating. At small L [Fig. 4a, curves (1) and (2)], the central part of the dependence $G(\delta)$ has a clearly pronounced

maximum, shifted towards negative δ values. With increasing L , the width of the central region decreases, and the height of the gain peak increases. At $L > 5 \mu\text{m}$, the central peak gradually transforms into a plateau, the width and height of which for long CNTs weakly depend on L [Fig. 4a, curve (3)]. For arrays with $L > 10 \mu\text{m}$, hitting the plateau region is ensured if δ/k_1 does not exceed ~ 0.15 in absolute value. The corresponding range of λ_2 values is $\sim 5 \text{ nm}$ (approximately from 1.029 to 1.034 μm).

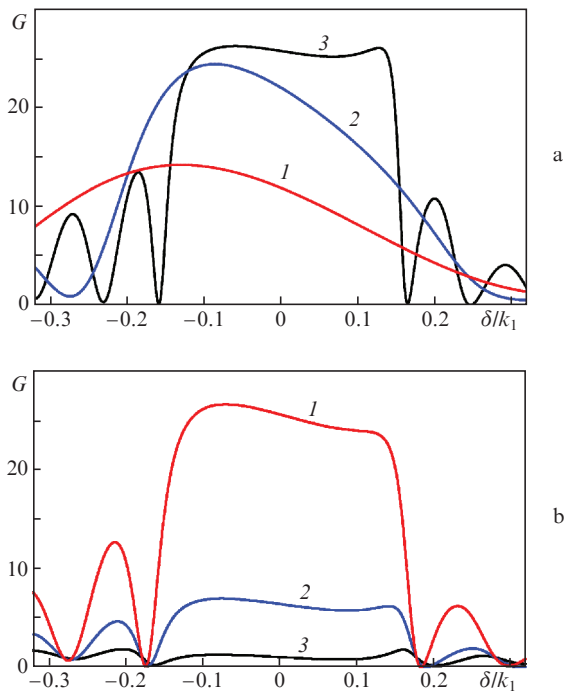


Figure 4. Dependences of the gain on the relative value of the phase detuning (a) at $\eta = 0.2$ and $L = (1) 2, (2) 4, (3) 10 \mu\text{m}$, as well as (b) at $L = 8 \mu\text{m}$ and $\eta = (1) 0.2, (2) 0.4, (3) 1.0$. The effective plasma frequency of the SWCNT array is taken to be 150 THz.

The curves in Fig. 4b correspond to different values of η (i.e., the input signal wave amplitude A_{20}) at a fixed $L = 8 \mu\text{m}$. Under optimal conditions (close to the phase matching regime at a sufficiently long interaction length L), the amplitude A_2 (regardless of its input value A_{20}) grows to a value of $\sim A_{10}$, taken as unity. Therefore, the maximum value of the gain G can be estimated as $(1/\eta)^2$. At $\eta = 1.0$ [curve (3)], the gain $G \approx 1$ and weakly depends on the parameter δ ; with a further increase in the ratio η , the value of G becomes less than unity, which means a transition to the inverse process of amplifying the wave with the frequency ω_1 at the expense of the energy carried by the wave with the frequency ω_2 .

4. Conclusions

We have shown that when two counterpropagating laser beams are incident on an array of parallel SWCNTs, one of the incident waves can be efficiently amplified due to the interaction with the counterpropagating wave of higher intensity and frequency. The gain depends on the geometric parameters of the structure (the length and radius of nanotubes, as well as the lattice period), amplitudes and frequencies of

waves. The frequencies of the interacting waves should differ by a small amount to ensure the most accurate fulfillment of the phase matching condition. In this case, of interest is the possibility of efficient reflection (with appropriate frequency conversion) of laser radiation in the near-IR range ($\lambda \approx 1 \mu\text{m}$) from a rarefied CNT array (with a period of more than 200 nm).

Reducing the length of the nanotubes that form the array makes it possible to expand the range of amplified frequencies, but the gain is somewhat reduced in this case. The maximum achievable gain is approximately equal to the square of the ratio of the pump and signal input amplitudes.

In conclusion, we note that for $\omega_1 < \omega_p$, the array under consideration operates as a metal mirror reflecting radiation at a layer thickness $L \approx \lambda_p = 2\pi c/\omega_p$, which is 1 μm or less. In this case, when the phase matching conditions are met, the irradiated array behaves in accordance with the results we obtained earlier in Ref. [26].

Acknowledgements. This work was supported by the Ministry of Science and Higher Education of the Russian Federation (Programme of Mega-Grants, application 2020-220-08-1369, Project No. 0004-2019-0002), and the Russian Foundation for Basic Research (Project No. 18-29-19101 mk).

References

- Garcia-Vidal F.J., Pitarke J.M., Pendry J.B. *Phys. Rev. Lett.*, **78**, 4289 (1997).
- Dai L., Patil A., Gong X., Guo Zh., Liu L., Liu Y., Zhu D. *Chem. Phys. Chem.*, **4**, 1150 (2003).
- Lidorikis E., Ferrari A.C. *ACS Nano*, **3**, 1238 (2009).
- Butt H., Dai Q., Farah P., Butler T., Wilkinson T.D., Baumberg J.J., Amaratunga G.A.J. *Appl. Phys. Lett.*, **97**, 163102 (2010).
- Bao H., Ruan X., Fisher T. *Opt. Express*, **18**, 6347 (2010).
- Nefedov I.S., Tretyakov S.A. *Phys. Rev. B*, **84**, 113410 (2011).
- Magesh Kumar K.K., Tripathi V.K. *Phys. Plasmas*, **20**, 092103 (2013).
- Gao W., Doiron C.F., Li X., Kono J., Naik G.V. *ACS Photonics*, **9**, 1602 (2019).
- Roberts J.A., Yu S.-J., Ho P.-H., Schoeche S., Falk A.L., Fan J.A. *Nano Lett.*, **19**, 3131 (2019).
- Hashemi S.M., Nefedov I.S. *Phys. Rev. B*, **86**, 195411 (2012).
- Liu X.L., Zhang R.Z., Zhang Z.M. *App. Phys. Lett.*, **103**, 213102 (2013).
- Hao J., Hanson G.W. *Phys. Rev. B*, **74**, 035119 (2006).
- Moradi A. *Chin. Phys. B*, **22**, 064201 (2013).
- Slepyan G.Ya., Maksimenko S.A., Lakhtakia A., Yevtushenko O.M., Gusakov A.V. *Phys. Rev. B*, **60**, 17136 (1999).
- Attia A.M. *Progr. Electromagn. Res.*, **94**, 419 (2009).
- Moradi A. *J. Electromagn. Anal. Applicat.*, **2**, 672 (2010).
- Moradi A. *Photonics Nanostruct. Fundam. Appl.*, **11**, 85 (2013).
- Martin-Moreno L., Garcia de Abajo F.J., Garcia-Vidal F.J. *Phys. Rev. Lett.*, **115**, 173601 (2015).
- Kadochkin A.S., Moiseev S.G., Dadoenkova Y.S., Svetukhin V.V., Zolotovskii I.O. *Opt. Express*, **25**, 27165 (2017).
- Moiseev S.G., Dadoenkova Yu.S., Kadochkin A.S., Fotiadi A.A., Svetukhin V.V., Zolotovskii I.O. *Ann. Phys.*, **530** (11), 1800197 (2018).
- Kadochkin A.S., Moiseev S.G., Dadoenkova Yu.S., Florian F.L.B., Svetukhin V.V., Zolotovskii I.O. *J. Opt.*, **22** (12), 125002 (2020).
- Nefedov I.S., Tretyakov S.A. *Photonics Nanostruct. Fundam. Appl.*, **9**, 374 (2011).
- Pendry J.B., Holden A.J., Stewart W.L., Youngs I. *Phys. Rev. Lett.*, **76**, 4773 (1996).
- Belov P.A., Marques R., Maslovski S.I., Nefedov I.S., Silverinha M., Simovski C.R., Tretyakov S.A. *Phys. Rev. B*, **67**, 113103 (2003).
- Maslovski S.I., Silverinha M.G. *Phys. Rev. B*, **80**, 245101 (2010).
- Afanas'ev S.A., Zolotovskii I.O., Kadochkin A.S., Moiseev S.G., Svetukhin V.V., Pavlov A.A. *Quantum Electron.*, **48** (9), 849 (2018) [*Kvantovaya Elektron.*, **48** (9), 849 (2018)].

27. Koroteev N.I., Shumay I.L. *Fizika moshchnogo lazernogo izlucheniya* (Physics of High-Power Laser Radiation) (Moscow: Nauka, 1991) pp 145–146.
28. Mayorov A.S., Elias D.C., Mukhin I.S., Morozov S.V., Ponomarenko L.A., Novoselov K.S., Geim A.K., Gorbachev R.V. *Nano Lett.*, **12**, 4629 (2012).
29. Yariv A., Yeh P. *Optical Waves in Crystals* (New York: Wiley, 1984).
30. Karpov S.Yu., Stolyarov S.N. *Phys. Usp.*, **36** (1), 1 (1993) [*Usp. Fiz. Nauk*, **163** (1), 63 (1993)].
31. Wei L., Wang Y.N. *Phys. Lett. A*, **333**, 303 (2004).
32. Nakanishi T., Ando T. *J. Phys. Soc. Jap.*, **78**, 114708 (2009).
33. Sasaki K., Murakami Sh., Yamamoto H. *Appl. Phys. Lett.*, **108**, 163109 (2016).
34. Miano G., Villone F. *IEEE Trans. Ant. Prop.*, **54**, 2713 (2006).